Biochimica et Biophysica Acta 1823 (2012) 808–817

Contents lists available at SciVerse ScienceDirect

Biochimica et Biophysica Acta

journal homepage: www.elsevier.com/locate/bbamcr

Identification of a nuclear carbonic anhydrase in *Caenorhabditis elegans*

Teresa A. Sherman [a], Sharath C. Rongali [a], Tori A. Matthews [a], Jason Pfeiffer [a], Keith Nehrke [a,b,*]

[a] Department of Medicine, University of Rochester Medical Center, Rochester, NY, USA
[b] Department of Pharmacology and Physiology, University of Rochester Medical Center, Rochester, NY, USA

ARTICLE INFO

Article history:
Received 17 October 2011
Received in revised form 1 December 2011
Accepted 13 December 2011
Available online 5 January 2012

Keywords:
Caenorhabditis elegans
Carbonic anhydrase
Nuclear targeting
pH regulation
Neurobiology

ABSTRACT

Background: Carbonic anhydrases (CA) catalyze the inter-conversion of CO_2 with HCO_3 and H^+, and are involved in a wide variety of physiologic processes such as anion transport, pH regulation, and water balance. In mammals there are sixteen members of the classical α-type CA family, while the simple genetic model organism *Caenorhabditis elegans* codes for six αCA isoforms (*cah-1* through *cah-6*).
Methods: Fluorescent reporter constructs were used to analyze gene promoter usage, splice variation, and protein localization in transgenic worms. Catalytic activity of recombinant CA proteins was assessed using Hansson's histochemistry. CA's ability to regulate pH as a function of CO_2 and HCO_3 was measured using dynamic fluorescent imaging of genetically-targeted biosensors.
Results: Each of the six CA genes was found to be expressed in a distinct repertoire of cell types. Surprisingly, worms also expressed a catalytically-active CA splice variant, *cah-4a*, in which an alternative first exon targeted the protein to the nucleus. *Cah-4a* expression was restricted mainly to the nervous system, where it was found in nearly all neurons, and recombinant CAH-4A protein could regulate pH in the nucleus.
Conclusions: In addition to establishing *C. elegans* as a platform for studying αCA function, this is the first example of a nuclear-targeted αCA in any organism to date.
General significance: A classical αCA isoform is targeted exclusively to the nucleus where its activity may impact nuclear physiologic and pathophysiologic responses.

1. Introduction

Carbonic anhydrases (CA, E.C. 4.2.1.1) are zinc-containing metalloenzymes (except for the ζ form, which utilizes cadmium instead) that catalyze the reversible hydration of carbon dioxide (CO_2) to bicarbonate ions (HCO_3^-) and protons (H^+). CA's are divided into several distinct classes (α, β (which likely includes the class previously categorized as ε), γ, δ and ζ), of which mammalian CAs belong to the α-class. To date, sixteen CA genes have been identified in humans, with isozymes distributed between the cytoplasm (CAI, II, III, VII, and XIII), the cell membrane (CAIV, IX, XII, and XIV), the mitochondria (CAVa and CAVb), and the extracellular space (CAVI) [1,2]. The CAXV gene is expressed in rodents, but appears to have become a pseudogene in primates [3]. Although most of the human CAs are catalytic, at least three of them (CAVIII, CAX, and CAXI) are not. Catalytic CA enzymes have two conserved features, a Zn^{2+} ion linked to a histidine triad through imidazoles [2] and a fourth histidine acting as a proton shuttle [4]. Gene products that are acatalytic appear to lack one or more of these features.

In animals, CAs participate in pH homeostasis, CO_2 and bicarbonate transport, water and electrolyte balance, and biosynthetic reactions; the precise role of individual CA isozymes is determined by their cellular and tissue expression, subcellular localization, and catalytic rate [5]. For example, mammalian CAII is an intracellular protein that is widely expressed, it has a fast rate of catalysis that has been deemed diffusion-limited, and its role in transport metabolons that link CA activity to HCO_3^- transporters has been suggested to maximize HCO_3^- membrane transport processes [6–10]. As such, it is not surprising that mutations in CAII have been linked to a variety of disorders including osteopetrosis, renal tubular acidosis and cerebral calcification [11]. In contrast, the expression of the GPI-anchored CAIV isozyme on the cell surface is thought to help buffer the extracellular space in the brains of mice [12] and CAIV has been shown to interact functionally with AE3 to mediate Cl^-/HCO_3^- exchange [13]. It is possible that this regulation of extracellular pH may contribute to synaptic excitability [14,15]. However, it is equally possible that a non-catalytic function of CAIV may contribute to its physiologic role in select cells, as recent data have suggested that the transport activity of the high-affinity monocarboxylate transporter MCT2 is enhanced by CAIV independent of the latter's catalytic activity

Abbreviations: AE3, anion exchanger 3; BSA, bovine serum albumin; CA, carbonic anhydrase; CHO, Chinese hamster ovary cells; GPI, glycosylphosphatidylinositol; GFP, green fluorescent protein; MCT2, monocarboxylate transporter 2; NLS, nuclear localization sequence; ORF, open reading frame; PBS, phosphate buffered saline; PCR, polymerase chain reaction; RACE, rapid amplification of cDNA ends; RNAi, double-stranded RNA mediated gene interference; RT, room temperature; SL1/SL2, trans-spliced leader sequences; SV40, Simian virus 40; UTR, untranslated region

* Corresponding author at: Department of Medicine, Box 675, University of Rochester Medical Center, 601 Elmwood Avenue, Rochester, NY 14642, USA. Tel.: +1 585 275 7020; fax: +1 585 442 9201.
E-mail address: keith_nehrke@urmc.rochester.edu (K. Nehrke).

0167-4889/$ – see front matter © 2012 Elsevier B.V. All rights reserved.
doi:10.1016/j.bbamcr.2011.12.014

[16]. Though CAIV has been shown to be expressed in a variety of tissue types, thus far CAIV mutational phenotypes have been limited to the retina [17].

In addition to their normal physiologic functions, alterations in CA expression have been correlated with pathologic conditions. For example, CAIX is regulated by hypoxia-inducible factor, hypoxia is a hallmark of many cancers, and CAIX has been shown to be elevated in many tumor types [18,19]. In fact, CAIX antibodies are useful as a diagnostic marker for tumors [20–23] and CAIX inhibition is currently being explored as a therapeutic strategy for cancer [24]. Similarly, acetazolamide, a classic CA inhibitor, is used to treat various diseases/disorders, including glaucoma [25], epileptic seizures [26], brain swelling following surgery [27], and altitude sickness [28].

Although CAs are widely studied, our understanding of them remains veiled. One of the most obvious gaps is a lack of knowledge as to the normal physiologic role of the acatalytic isoforms. The genome of the model organism *Caenorhabditis elegans* codes for six α-CA isoforms (*cah-1*, *2*, *3*, *4*, *5* and *6*), and three of these lack the necessary components for catalytic activity (*cah-1*, *2* and *6*). Thus, *C. elegans* may be a useful reductionist model for discerning the function of both catalytic CAs as well as the evolutionarily conserved acatalytic proteins. Previously, the temporal expression patterns of the worm CA gene family have been studied [29] and one of these genes, *cah-4*, has been shown to be regulated by both environmental pH [30] and oxygen levels [31]. *Cah-4* may also play a role in the progression of muscle degeneration in a worm model of muscular dystrophy [32].

Here, we experimentally defined the transcripts arising from the six *cah* genes in worms, including their usage of alternative promoters and splice variation. We generated transgenic nematodes to determine the gene expression patterns and intracellular location of the six worm *cah* gene products, as well as how splice variation affected protein targeting. In addition, we expressed the *C. elegans cah* cDNAs and their splice variants in mammalian tissue culture cells, then assessed protein localization and activity, respectively.

To our surprise, we found a splice variant of *cah-4*, the same gene implicated by three separate groups as being physiologically important [30–32], that was targeted to the cell nucleus. Nuclear expression, which required a 45 amino acid N-terminal extension coded for by an alternative first exon, occurred nearly exclusively and ubiquitously throughout the nervous system. Though an RNA splicing factor has previously been shown to have catalytic CA activity [33], our results are the first to demonstrate that a classical αCA resides in the nucleus of any organism. Both of the *cah-4* splice variants were found to be catalytically active, and we hypothesize that CAH-4A may contribute to nuclear pH regulation or oxidative stress resistance.

In conclusion, the results presented here form a foundation upon which to structure genetic approaches using a powerful model system to identify new functions for a widespread, evolutionarily-conserved gene family.

2. Methods

2.1. C. elegans strains

Nematodes were routinely cultured at either 16 °C or 20 °C on Normal Growth Media agar plates seeded with OP50 bacteria. To create transgenic lines, young adult worms (generally *pha-1*(*e2123ts*)III mutants) grown at the permissive temperature of 16 °C were microinjected with DNA at a final concentration of 150 ng/μl in high-potassium injection buffer [34]. In general, equal amounts of experimental DNA and rescue marker (pCL1, a vector coding for *pha-1*) were co-injected. In some cases, over-expression of GFP-tagged CA was toxic to worms, and in these cases the amount of experimental DNA in the injection mix was reduced.

The strains developed and reported on in this work are:

Transcriptional fusions (referred to in the figures as P*genename*::GFP) — KWN333, *pha-1*(*e2123ts*)III rnyEx199 [P*cah-1*::GFP PCR; pCL1 (*pha-1*+)]; KWN334, *pha-1*(*e2123ts*)III rnyEx200 [P*cah-2a*::GFP PCR; pCL1 (*pha-1*+)]; KWN335, *pha-1*(*e2123ts*)III rnyEx201 [P*cah-2b*::GFP PCR; pCL1 (*pha-1*+)]; KWN336, *pha-1*(*e2123ts*)III rnyEx202 [P*cah-3*::GFP PCR; pCL1 (*pha-1*+)]; KWN337, *pha-1*(*e2123ts*)III rnyEx203 [P*cah-5*::GFP PCR; pCL1 (*pha-1*+)]; KWN338, *pha-1*(*e2123ts*)III rnyEx204 [P*cah-6*::GFP PCR; pCL1 (*pha-1*+)].

Translational fusions (referred to in the figures as P*genename*::PROTEIN::GFP) — KWN339, *pha-1*(*e2123ts*)III *him-5*(*e1490*)V, rnyEx205 [P*cah-5*::CAH-5::pHluorin PCR; pCL1 (*pha-1*+)]; KWN340, *pha-1*(*e2123ts*)III *him-5*(*e1490*)V, rnyEx206 [P*cah-3*::CAH-3::GFP PCR; pCL1 (*pha-1*+)]; KWN348, *pha-1*(*e2123ts*)III *him-5*(*e1490*)V, rnyEx213 [P*cah-1*::CAH-1::GFP PCR; pCL1 (*pha-1*+)]; KWN349, *pha-1*(*e2123ts*)III *him-5*(*e1490*)V, rnyEx211 [P*cah-2b*::CAH-2B::GFP PCR; pCL1 (*pha-1*+)]; KWN350, *pha-1*(*e2123ts*)III *him-5*(*e1490*)V, rnyEx214 [Pcah-6::CAH-6::GFP PCR; pCL1 (*pha-1*+)]; KWN351, *pha-1*(*e2123ts*)III *him-5*(*e1490*)V, rnyEx215 [P*cah-2a*::CAH-2A::GFP PCR; pCL1 (*pha-1*+)].

Cah-4 fusions: KWN172, *pha-1*(*e2123ts*)III *him-5*(*e1490*)V, rnyEx096 [P*cah-4a*::GFP PCR; pCL1 (*pha-1*+)]; KWN35, *pha-1*(*e2123ts*)III *him-5*(*e1490*)V rnyEx013 [pIA3-R01a (P*cah-4a*::CAH-4A::GFP), pCL1 (*pha-1*+)]; KWN36, *pha-1*(*e2123ts*)III *him-5*(*e1490*)V rnyEx014 [pIA3-R01b (P*cah-4b*::CAH-4B::GFP), pCL1 (*pha-1*+)]; KWN377, *pha-1*(*e2123ts*)III rnyEx232 [P*cah-4a*::GFP::CAH-4A PCR, pCL1 (*pha-1*+)]; KWN378, *pha-1*(*e2123ts*)III rnyEx233 [pKT23 (P*nhx-2*::CAH-4A exon 1::GFP), pCL1 (*pha-1*+)].

2.2. Molecular techniques

2.2.1. 5′ and 3′ RACE

Random hexamer primers were used to synthesize cDNA from a mixed-stage population of *C. elegans* using an iScript Tm cDNA synthesis kit (BioRad, Hercules, CA). Nested gene-specific oligonucleotides were then employed in consecutive rounds of PCR in combination with an adaptor primer for 3′ RACE or SL1/SL2 leader primers for 5′ RACE (almost all *C. elegans* mRNAs have a non-template encoded 5′ trans-spliced 22 nt leader added post-transcriptionally, with SL2 leaders being good indicators of the ~15% of worm genes that are downstream in an operon). Each individual PCR product was gel-isolated, cloned, and sequenced.

2.2.2. cDNA expression and detection

The predicted ORFs for each *cah* gene product were cloned from gel-isolated PCR fragments into the vector pcDNA3.1-V5/His/topo (Invitrogen, Carlsbad, CA) to create pcDNA3.1*cah-1* through pcDNA3.1*cah-6*. Each insert was fully sequenced on both strands and was engineered to lack the endogenous stop codon. Instead, a V5 epitope was encoded in-frame at the C-terminus of each ORF; this epitope was recognized by a commercially available mouse monoclonal anti-V5 antibody (Invitrogen). CHO cells that had been transiently transfected with the *cah* expression vectors were fixed in PBS/2% paraformaldehyde/50% methanol for 20 min at 4 °C, then permeabilized and blocked in PBS/0.1% Triton X-100/5% BSA/1% Normal Goat Serum for 1 h at RT prior to antibody incubation (1:2000 dilution in blocking buffer). Following 3× washes in PBS/0.1% Triton X-100, the anti-V5 antibody was detected using a 1:5000 dilution of rabbit anti-mouse IgG conjugated to Alexa Fluor 488.

The rabbit CAIV expression vector was a kind gift of Dr. George Schwartz (Univ. of Rochester).

2.2.3. GFP fusions

In order to create transcriptional and translational fusions of the *cah* promoters and genomic ORFs to GFP for expression in transgenic worms, PCR sewing was used. In short, a PCR product amplified from *C. elegans* genomic DNA was engineered with a non-template

encoded 5′ extension built into one of the oligonucleotides such that it was complementary to the 5′ end of a separate PCR product coding for GFP (with the *unc-54* 3′ UTR added for mRNA stability). The two PCR products were gel-isolated, combined, and allowed to progress through five rounds of PCR amplification in the absence of primers, resulting in the annealing and extension of the two products. Prior to the sixth round of amplification, a 5′ nested primer targeted at the promoter::ORF product and a 3′ nested primer targeted at the *unc-54* 3′ UTR product were added and the reaction was allowed to progress for an additional 20 cycles. The final full length product was phenol/chloroform extracted, precipitated with ethanol, and used for microinjection. The sizes of the promoter fragments used to drive expression in the PCR fusions were: *cah-1*, 3470 nt; *cah-2a*, 1399 nt; *cah-2b*, 1610 nt; *cah-3*, 3319 nt; *cah-4a*, 348 nt; *cah-4b*, 3286 nt; *cah-5*, 3056 nt; *cah-6*, 3531 nt.

2.2.4. Cah-4 vectors

Standard molecular cloning techniques were used. The vector pKT23 (P*nhx-2*::CAH-4A EXON 1::GFP) was created by PCR amplification of the 45 amino acid coding region found in the first exon of *cah-4a* using Acc65I-tagged primers, followed by digestion and cloning into the Acc65I site of pIA5-nhx-2 [35]. The vectors pIA3-RO1a and pIA3-RO1b were likewise created by PCR, using *C. elegans* genomic DNA as a template. pIA3-RO1a contains a region from immediately downstream of the first (non-coding) exon in *cah-4b* to the end of the *cah-4* coding region, cloned in frame with GFP in the base vector pIA3 [35] as an *Nhe*I-*Sac*II fragment. pIA3-R01b contains the *cah-4b* promoter cloned as an *Nhe*I-*Sac*II fragment into pIA3, with the *cah-4b* coding region then cloned as a *Sac*II fragment into the resulting vector. This effectively removed the *cah-4a* promoter and first exon from the construct.

2.2.5. NLS-pHluorin vector

pKT18 was created by PCR cloning the ratiometric fluorescent biosensor pHluorin cDNA [36] amplified using a primer containing a 5′ non-template encoded SV40 NLS into the topo TA cloning vector pcDNA3.1 V5/His/topo (Invitrogen Corp., Carlsbad, CA). The insert was fully sequence on both strands.

2.3. Dynamic fluorescent imaging

pKT18 was transiently transfected into CHO cells in culture using Lipofectamine 2000 (Invitroge., Carlsbad, CA) as recommended by the manufacturer. Immediately following transfection, cells were trypsinized onto glass coverslips and allowed to adhere under normal growth conditions overnight. The following day, a coverslip containing adherent cells was placed into a perfusion chamber residing on the stage of a Nikon Eclipse 2000 inverted microscope (Nikon Instruments Inc., Melville, NY) equipped with a monochromator (TILL Photonics, Germany) and Cooke sensicam (Cooke Corp., Romuslus, MI) running TILLvisION software for image acquisition. The cells were superfused with buffer containing HCO_3^- (in mM): 115 NaCl, 20 $NaHCO_3^-$, 5.4 KCl, 0.4 KH_2PO_4, 0.33 NaH2PO_4, 10 glucose, 20 Hepes, 1.2 $CaCl_2$, 0.8 $MgSO_4$, bubbled with 5% CO_2 and adjusted to pH 7.4 with Tris. Following equilibration, the cells were switched to a HCO_3^- free buffer (in mM): 135 NaCl, 5.4 KCl, 0.4 KH_2PO_4, 0.33 NaH_2PO_4, 10 glucose, 20 Hepes, 1.2 $CaCl_2$, 0.8 $MgSO_4$, pH adjusted to 7.4 with Tris base. During this period, 535-nM emissions were measured following excitation at either 410-nm or 470-nm, and the ratio of these emissions was converted to pH by in situ calibration using the high K+/nigericin technique [37].

2.4. Hansson's technique

CHO cells were plated onto glass coverslips and transiently transfected with pcDNA3.1-based mammalian expression vectors coding for V5 epitope-tagged CAH proteins using Lipofectamine 2000 (Invitrogen). 24-hours post-transfection, the cells were fixed and stained for CA activity using a cobalt–phosphate detection method [38]. Briefly, the cells were incubated overnight at 4 °C in 3% glutaraldehyde in 0.1 M sodium phosphate buffer pH 7.3 to fix. Following three rinses with 0.1 M sodium phosphate buffer (pH 7.3), the cells were incubated for 5 min in a solution made by combining 17 ml of solution A (containing 1 ml of 0.1 M CoSO4, 6 ml of 0.5 M H2SO4 and 10 ml of 0.066 M KH2PO4) with 40 ml of solution B (0.75 g of NaHCO3 in 40 ml of ddH2O). Each of these solutions was prepared fresh from stocks as indicated. The cells were then rinsed in 0.1 M sodium phosphate buffer (pH 7.3), and incubated in freshly-made 0.5% $(NH_4)2S$ for 2 min. The reaction was halted by rinsing with ddH2O. To control for non-enzymatic CA activity, the cells were pre-incubated in 10^{-4} M acetazolamide for 2 h.

3. Results

3.1. The cah family in worms

An in silico analysis based upon conserved regions from the mammalian αCA family indicated that the *C. elegans* genome contains the coding potential for six αCA isoforms. 5′ and 3′ Rapid Amplification of cDNA Ends (RACE) was used to experimentally determine the products arising from transcription of these six putative genes. Two rounds of RACE were performed using nested gene-specific primers designed based upon the predicted DNA sequences in well-conserved regions of the putative ORFs. 3′ RACE products were amplified using an adaptor primer that was tagged onto the dT18 primer used during cDNA synthesis, while 5′ RACE products were amplified using upstream primers corresponding to either SL1 or SL2 trans-spliced leader sequences, which are 22 nucleotide RNAs that are added post-transcriptionally to most genes in worms. All of the major products arising from these reactions were purified, cloned, sequenced and aligned to a genomic map to determine transcriptional start sites and splice variation.

A schematic of our results, including the exons (shown in black), 5′ and 3′ UTR regions (shown in gray), and leader sequences (SL1) is drawn to scale (in kb) in Fig. 1A. As indicated, each of the six *cah* gene products was found to be trans-spliced to an SL1 leader, and there was no evidence of SL2 splicing (data not shown). SL2 leaders are generally restricted to the <15% of transcripts in worms that occur in operons. As is often the case with worm transcripts, each of the genes contained very short 5′ UTRs, while the 3′ UTRs were of varying length. In addition, two splice variants were identified for the *cah-2* and *cah-4* genes. This variation occurred at the 5′ ends and resulted in alternative first exons. For both *cah-2* and *cah-4*, transcription of the downstream splice variant was driven by a promoter contained within the first intron of the upstream splice variant, as indicated (Fig. 1A).

Protein sequences were determined by virtual translation of the *cah* ORFs, which were then aligned to the CA isozymes from mammals. The slanted cladogram in Fig. 1B indicates the relatedness between the six *cah* αCAs from *C. elegans* and CAI through CAXIV from humans (with CAXV being a pseudogene). Interestingly, the CAs cluster into three distinct groups. These include soluble isozymes, membrane-associated isozymes, and acatalytic isozymes. *Cah-1*, *cah-2*, and *cah-6* are found in a clade with the acatalytic isozymes, which is not unexpected given their lack of certain residues necessary for catalytic activity. *Cah-3* and *cah-5* are most closely associated with the soluble, catalytic human isozymes. *Cah-4* is more closely related to the catalytic isozymes. Not surprisingly given the expansion of the CA gene family in mammals, the cladogram in Fig. 1B does not predict direct orthologs and the closest relationship between the *C. elegans* and human CAs are found amongst the acatalytic isozymes. There is little known as to the molecular function of this sub-class of CA isozyme in mammals, but the intriguing

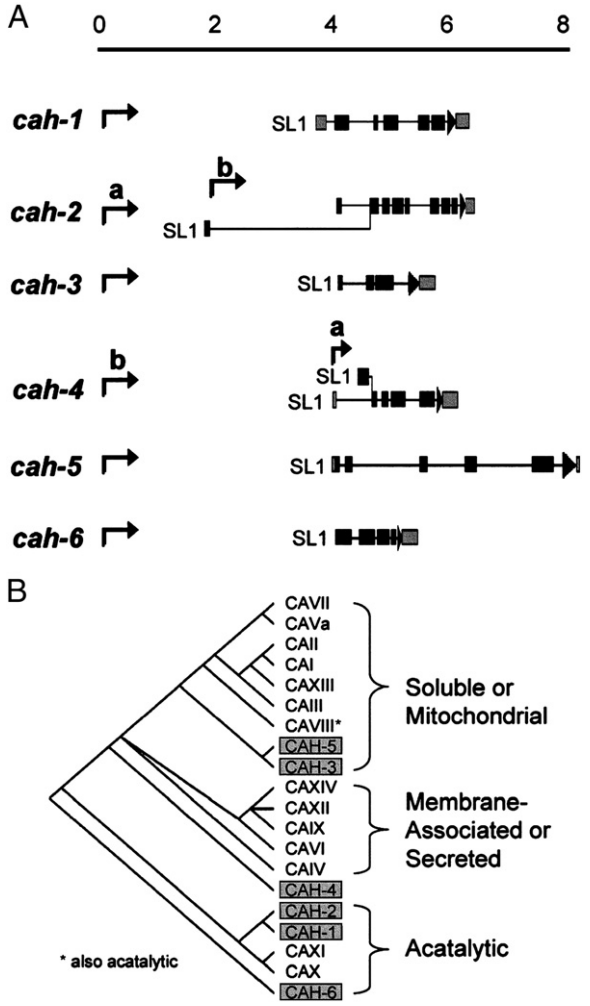

Fig. 1. The *C. elegans* genome codes for six alpha carbonic anhydrase isoforms. (A) Schematic of the experimentally-defined intron-exon structures for six *cah* genes, drawn to scale (in kb). Coding exons are shown in black, while 5′ and 3′ UTRs are shown in gray. SL1 leader trans-splice sites are as indicated. The promoter regions used to determine expression patterns for each isoform and splice variant are denoted by arrows. (B) Slanted cladogram indicating the relatedness between the six *cah* alpha carbonic anhydrase gene products from *C. elegans* and representative CA isoforms from humans. The outgroup-rooted map was generated using UPGMA tree building with Poisson distance correction, running in bootstrap mode. Each of the six nematode carbonic anhydrases is highlighted by gray shadowing. Gene products that are clustered in the "acatalytic" group (as well as CAVIII) lack a triad of histidines that is required for metal ion coordination and activity.

observation that half of the αCAs are presumably acatalytic in *C elegans* suggests an evolutionarily conserved and potentially important biologic purpose.

3.2. Cellular expression patterns and intracellular location of the cah gene products

To better understand the physiologic role of each of the six *cah* gene products in worms, we determined where they were expressed. Genomic PCR products containing the *cah* promoter regions were used to drive the transcription of GFP in transgenic worms, and GFP expression was assessed by fluorescent microscopy. The genomic regions used as promoters are denoted by arrows in Fig. 1A.

Neuronal expression was observed in all transgenic lines (Fig. 2). In most cases only subsets of the 302 adult neurons expressed GFP, but in at least two cases, *cah-6* (Fig. 2) and *cah-4a* (Fig. 3D), expression appeared to occur throughout the entire nervous system. In addition to neuronal labeling, strong expression was observed in the intestine (Fig. 2; *cah-2a*, *cah-3*, and *cah-5*), the hypodermis (Figs. 2 and 3E; *cah-4b* and *cah-5*), and various muscle cells including the vulva and pharynx (Figs. 2 and 3; *cah-2a*, *cah-3*, *cah-4a*, *cah-4b*, and *cah-5*). A synopsis of these expression patterns can be found in Table 1. This list is not inclusive, but does detail the major cell types and organs where expression of each isoform was observed. Two caveats are that promoter-driven GFP expression from transgenic extrachromosomal arrays only approximates endogenous gene expression, and the expression of genes from arrays is suppressed in the *C. elegans* germline.

In order to establish the intracellular residence of each CA isozyme, the promoters and ORFs were fused to GFP in lieu of the endogenous stop codon by PCR sewing, and the PCR products were injected into worms to create transgenic lines. Fluorescent images of these lines confirmed the cellular expression profiles established above, and helped to clarify protein localization (Fig. S1; Table 1). One important caveat here is that it is unclear whether these GFP fusion proteins are functional, and as with all transgenic and fusion protein analysis, the results need to be interpreted in this context.

Most of the isozymes that were predicted to be catalytic were found in the cytoplasm (Fig. S1 and Fig. 3; *cah-3*, *cah-4b*, and *cah-5*). Two of the putative acatalytic isozymes were intracellular but punctate (Fig. S1; *cah-1* and *cah-2*). These punca did not co-localize with the mitochondrial label MitoTracker Red CMXRos and reducing the concentration of the transgenes in the injection mix by 1:30 gave similar results, which led us to believe that they are not merely due to non-specific protein aggregation (data not shown) The final acatalytic isozyme was associated with areas where neurons make contact with other cells, including synapses and neuromuscular junctions (Fig. S1; *cah-6*). We found no evidence for a mitochondrial CA such as mammalian CAV, nor did we detect either extracellular or membrane-bound CA in worms. While this is not a conclusive proof that such an isozyme does not exist, it is suggestive.

The most unexpected finding was the discovery of a nuclear CA isozyme (Fig. 3; *cah-4a*). The *cah-4* gene contains two alternative first exons whose expression is driven by distinct promoters (Fig. 1). The only difference between the resulting proteins is a 45 amino acid region immediately following the initiator Met in CAH-4A that is absent in CAH-4B. While a *cah-4b* translational fusion protein was expressed most strongly in the excretory cell, GFP labeling was also found in the cytoplasm of various muscle and hypodermal cells (Fig. 3B). In contrast, the *cah-4a* promoter was expressed throughout the nervous system as well as in the head muscle cells (Fig. 3D), and a translational CAH-4A::GFP fusion protein was apparently directed to the nucleus of these cells (Fig. 3F). In head muscle cells, unlike neurons, the nuclei are small compared to the overall cell size, and nuclear targeting was readily observable. We also confirmed that GFP fluorescence in neurons co-localized with DAPI staining in the nucleus (Fig. S2).

Moving GFP from the C-terminus to the N-terminus of CAH-4A demonstrated that exon 1 was not strictly an N-terminal sorting signal and that it could drive nuclear localization from a site within the fusion protein (Fig. 4A). In fact, 45 amino acids coded for by exon 1 formed a bona fide NLS which on its own was sufficient to direct GFP to the nucleus (Fig. 4B). This targeting was not limited to neurons, either, as an exon 1::GFP fusion that was driven by the *nhx-2* promoter was found in the nucleus of intestinal cells (Fig. 4C). Thus, we conclude that CAH-4A is a nuclear CA, and we hypothesize that it contributes to neuronal function through a previously-unrecognized role in nuclear physiology.

3.3. Immunodetection and catalytic activity of recombinant CAs

To test for catalytic activity of the worm CAs, their ORFs were cloned and expressed as recombinant V5 epitope-tagged proteins in CHO cells. Anti-V5 antibody staining was used to assess recombinant protein targeting, while Hansson's histochemistry was used to assay catalytic activity. Hansson's stain is a cobalt precipitate that results

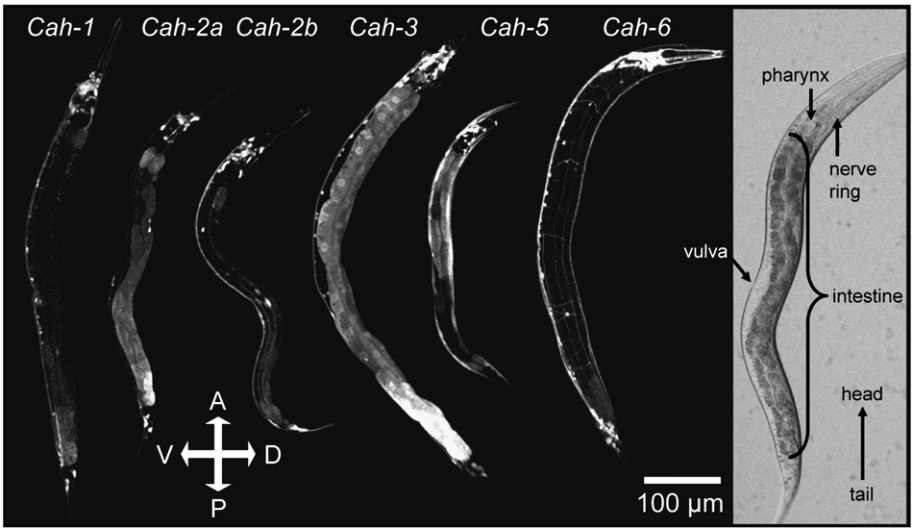

Fig. 2. *Cah* gene expression patterns. Representative confocal maximum projection images are shown of worms (L4-adult) from each of six transgenic strains expressing promoter::GFP fusions corresponding to the genes indicated. A single DIC micrograph shows physiologic structure and the major organs are labeled. The white arrows indicate orientation (a, anterior; p, posterior; d, dorsal; v, ventral). A summary of tissues where each *cah* promoter is active can be found in Table 1.

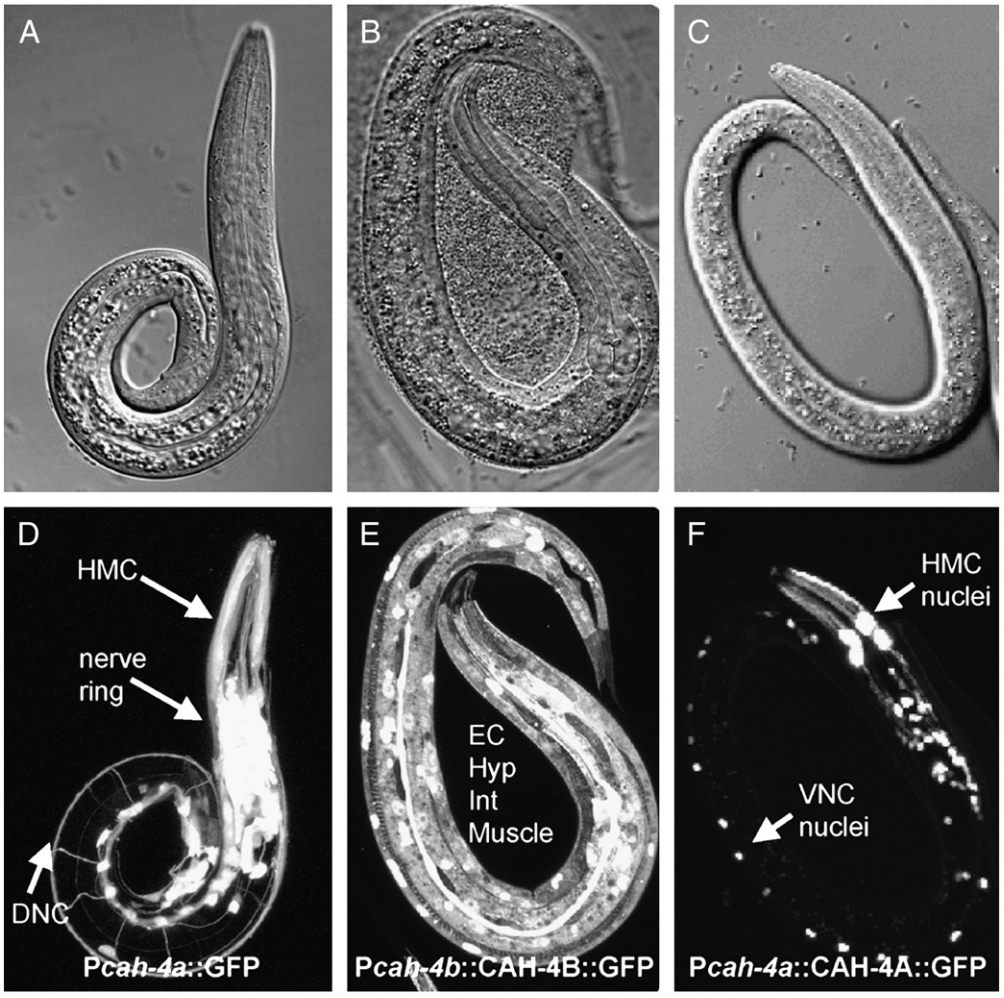

Fig. 3. *Cah-4* codes for both cytoplasmic and nuclear carbonic anhydrase isoforms. Representative DIC (A–C) and fluorescent maximum projection confocal micrographs (D–F) of transgenic strains expressing promoter::ORF::GFP fusions, as indicated. Where possible, arrows have been used to indicate the relevant cells and cell groups. (A, D) The intra-exonic *cah-4a* promoter drives GFP expression throughout the nervous system, as well as in head muscle cells. (B, E) The *cah-4b* promoter is active in a variety of tissues, including the excretory cell, body wall muscle, hypodermis, seam cells, and the intestine, but is not expressed in neurons. These cells comprise most of the body architecture and are thus not indicated by individual arrows. The CAH-4B::GFP fusion protein resides in the cytoplasm. (C, F) The CAH-4A::GFP fusion protein is targeted primarily to the nucleus, as is most readily apparent in the head muscle cells. HMC, head muscle cell; DNC, dorsal nerve cord; EC, excretory cell; Hyp, hypodermal cells; Int, intestine; VNC, ventral nerve cord.

Table 1
Expression patterns of *cah* isoforms.

Gene	Cell type | localization
Cah-1	Neurons (++) | intracellular puncta
Cah-2a	Neurons (+), Intestine | intracellular puncta
Cah-2b	Neurons (+), vulva | intracellular puncta
Cah-3	Neurons (++), intestine, pharynx | cytoplasm
Cah-4a	Neurons (+++), head muscle, vulval muscle | cytoplasm
Cah-4b	Excretory cell, body wall muscle, intestine, hypodermis, anal muscle | nucleus
Cah-5	Neurons (+), intestine, body wall muscle, hypodermis | cytoplasm
Cah-6	Neurons (+++) | synapses and neuromuscular junctions

from CA activity and serves as a visual indicator of both catalytic potential and the location of catalysis [38].

As a positive control, cells were transfected with rabbit CAIV, a GPI-anchored extracellular CA that stains at cell–cell contacts when reacted with Hansson's (Fig. 5D). As expected, despite being anti-V5 immuno-reactive, cells transfected with *cah-1*, *cah-2* or *cah-6* cDNAs were not stained by Hansson's technique (data not shown). However, cells transfected with *cah-3*, *cah-4a* or *cah-4b* cDNA were robustly stained (Fig. 5E–G). In the case of *cah-4a*, the staining was predominantly nuclear (Fig. 5G). This result also confirmed previous data indicating that the CAH-4B isozyme was catalytic [30]. Each of these three CA isozymes' activities was inhibited by preincubation with 10 μM acetazolamide (data not shown). Interestingly, we found that CAH-5, though expressed in the cytoplasm, did not result in discernable CA activity using Hansson's technique (data not shown). This isozyme may have a very low catalytic activity or specific requirements that are not met in this assay.

Cells that expressed either *cah-3* or *cah-4b* cDNA were anti-V5 antibody reactive in both the cytoplasm and the nucleus (Fig. 5A and B), while cells that expressed *cah-4a* cDNA were reactive strictly in the nucleus (Fig. 5C). We attribute the partial nuclear distribution of the CAH-3 and CAH-4B proteins to the fact that they are quite small (~30 kDa) and may passively diffuse through the nuclear pore, as well as the fact that the nuclei in these cells are thicker than the cytoplasm, leading to what can appear to be nuclear enrichment when viewed by epifluorescent microscopy. GFP fusion proteins such as shown in Fig. 2 are likely beyond the molecular weight range within which free diffusion might occur. Even so, the results shown in Fig. 4 are consistent with active targeting of CAH-4A to the nucleus, as very little cytoplasmic signal was observed with either immunodetection or Hansson's staining.

3.4. CAH-4A influences HCO3- mediated changes in nuclear pH

CAs can contribute to pH regulation both inside and outside of the cell. We next tested whether CAH-4A, consistent with its catalytic

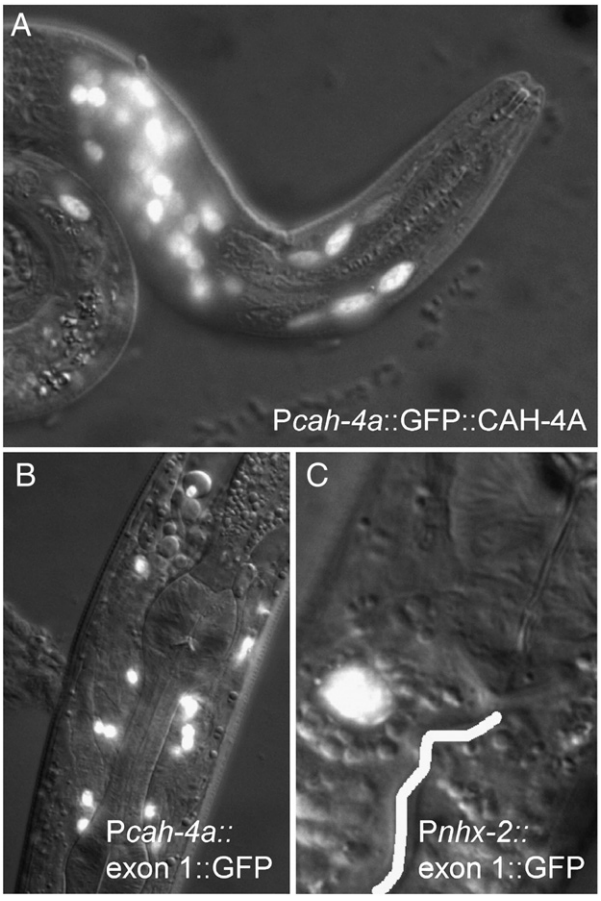

Fig. 4. Exon 1 of *cah-4a* codes for a nuclear localization sequence. DIC/fluorescent overlays of transgenic worms expressing various promoter::ORF::GFP configurations, as follows: (A) The *cah-4a* promoter, with the GFP fused to the N-terminus of CAH-4A rather than the C-terminus. (B) The *cah-4a* promoter, with the 45 amino acids coded for by exon 1 of *cah-4a* fused to the N-terminus of GFP. (C) The intestine-specific *nhx-2* promoter, with exon 1 of *cah-4a* fused to GFP as above.

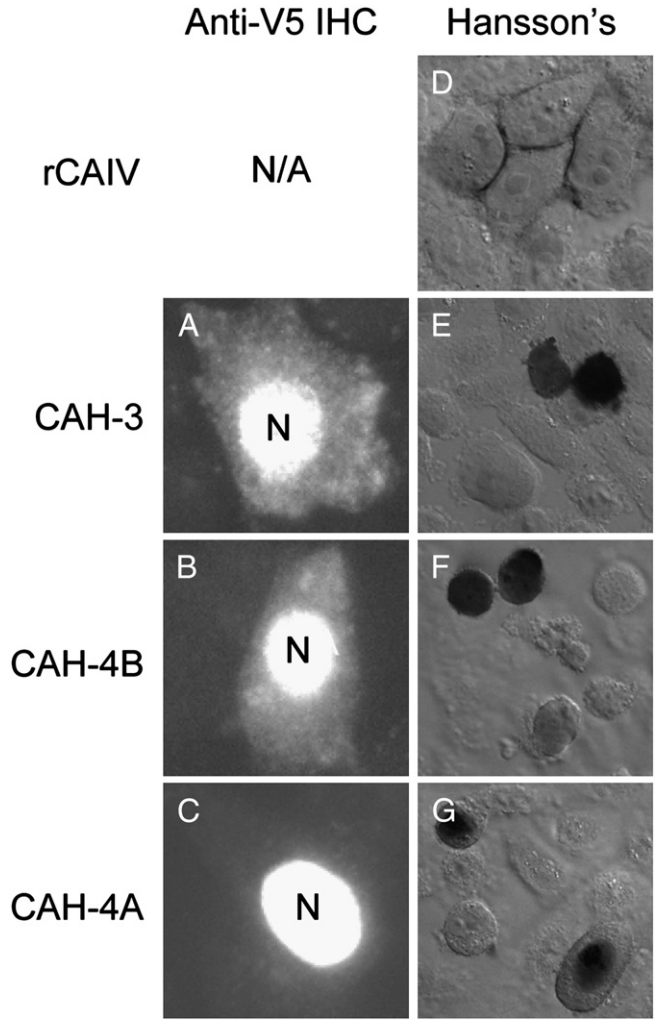

Fig. 5. Recombinant carbonic anhydrase activity and protein localization in mammalian tissue culture cells. (A–C) Fluorescent micrographs showing immunolocalization of V5 epitope-tagged CAH proteins expressed transiently in CHO cells (N, nuclei). (D–G) Transmitted light images of CHO cells stained using Hansson's histochemistry to detect carbonic anhydrase activity. Of the six *cah* genes tested, only the *cah-3* and *cah-4* gene products had a catalytic rate sufficient to observe reaction product. Rabbit CAIV served as a positive control; CAIV is a GPI anchored protein whose activity is limited to the cell periphery.

potential, could contribute to pH regulation in the nucleus. Nuclear pH was measured using dynamic fluorescent imaging of the pH-sensitive biosensor pHluorin, which was targeted to the nucleus via an SV40 NLS. Cells were allowed to equilibrate in 20 mM HCO_3^-–5% CO_2-buffered solution. Following equilibration, washout of CO_2 was brought about by switching perfusion to nominally HCO_3^-–CO_2-free solution. This caused a rapid alkalinization whose rate was dependent upon the conversion of HCO_3^- to CO_2. Consistent with the results of Hansson's staining, CHO cells expressing CAH-4A exhibited an increased rate of alkalinization compared to control cells following switchover (Fig. 6A). In addition, these cells exhibited an elevated resting nuclear pH. Acetazolamide reduced the rate of pH change in CAH-4A expressing cells to a value comparable to that of control cells, but had little effect on the rate in control cells themselves (Fig. 6B). We also found that expression of CAH-4B could accelerate the rate of nuclear pH change, though to a lesser extent than CAH-4A, consistent with its partial nuclear distribution in cultured cells (data not shown). To what extent this is an overexpression artifact is currently unknown. These results highlight the potential of a nuclear CA to contribute to organelle pH regulation. This ability may be particularly relevant in response to changes in HCO_3^-–CO_2 such as might result from cell metabolism or ischemic stress conditions.

4. Discussion

The mammalian CAs form a large family of zinc-containing metalloenzymes, and individual CAs have been shown to participate in pH regulation, HCO_3^- and ion transport, water and electrolyte balance, and photosynthesis and respiration [2,39,40]. As might be predicted, CA gene expression and protein distribution contribute to their particular physiologic roles. For example, mitochondrial CAV in the liver fuels pyruvate carboxylase and carbamoyl-phosphate synthetase, thus contributing to gluconeogenesis and the urea cycle, respectively [41,42]. Similarly, salivary CAVI, the only secreted isozyme in this enzyme family, is thought to help prevent dental plaque by reducing acidity in the oral cavity [43,44]. Further, membrane-bound CAIV and XIV isozymes contribute to extracellular pH buffering in the central nervous system [12].

The three acatalytic CA isozymes CAVIII, CAX, and CAXI are quite closely related to their active neighbors, and point mutations in the coding regions have been shown to be sufficient to convert a catalytically inactive protein to one with enzymatic CA activity [45,46]. However, very little is known about their physiologic function (for review, see [1]). Several intriguing observations regarding CAVIII have been reported: first, like the catalytically active CA IX and XII isozymes, CAVIII is overexpressed in certain cancers [47] and its expression can promote cancer cell growth and invasiveness; second, CAVIII is present in Purkinje cells, cerebellar nuclei and brainstem [48]; and third, a *Car8* mutant mouse (*wdl*) has a gait disorder and aberrant synaptic morphology in the cerebellum [49]. Since CAVIII has been identified as a binding partner for the inositol trisphosphate receptor and regulates its affinity for substrate [50], it is possible that the phenotype is related to calcium signaling in the cell.

Interestingly, in *C. elegans* three of the six αCA isozymes are predicted to be acatalytic based upon their lacking one or more of the conserved histidines required for Zn^{2+} binding, and our observations using Hannson's staining confirm this prediction. This suggests that CAs may have a conserved function independent of their role in CO_2 metabolism. Large scale RNAi screens have failed to identify a phenotype associated with the loss of any of these three isoforms, but the acatalytic isozymes are expressed mainly in neurons (Table 1), and neurons are typically refractory to RNAi. A more rigorous approach will involve creating deletion alleles for the acatalytic CA genes. In this regard, a strain containing a *cah-1* deletion allele (ok2032) has been developed by the *C. elegans* Gene Knockout Consortium and is viable as a homozygous null, but is presently uncharacterized.

In general, the cell expression patterns that we observed for the worm CA genes (Fig. 2 and Table 1) were similar to those described in a recent report [51]. However, our analysis of protein localization using translational GFP fusions provided some additional details of interest. First, based upon the distribution of the CA isozymes and the lack of an overt mitochondrial leader sequence on any of the catalytic variants, we conclude that worms lack a CAV ortholog. Second, the acatalytic isozyme CAH-6 localized to regions of cell–cell contact, including neuromuscular junctions (Fig. S1). While the fluorescent resolution was insufficient to determine whether the signal was associated with vesicles inside the cell or the plasma membrane, the pan-neural expression and specific targeting of this CA to synapses suggest that it may play a role in neurotransmission. Given that CAH-6 is one of the acatalytic isozymes, further dissection of its role in neurons may help to shed light on this under-studied sub-class of CAs. Finally, while it has been recognized that the *cah-4* gene codes for two alternate splice variants [30] whose expression is driven by mutually exclusive promoters (Fig. 3), our results demonstrated that this splicing generates a CA isozyme containing a 45 amino acid N-terminal extension that is both necessary and sufficient for CAH-4A protein targeting to the cell nucleus (Fig. 4). This is the first example of a CA in any organism that resides in the nucleus, and begs the question of what the physiologic role of a nuclear CA might be.

While *cah-4b* is expressed in hypodermis, excretory cell and muscle, the *cah-4a* promoter drives expression throughout the nervous system,

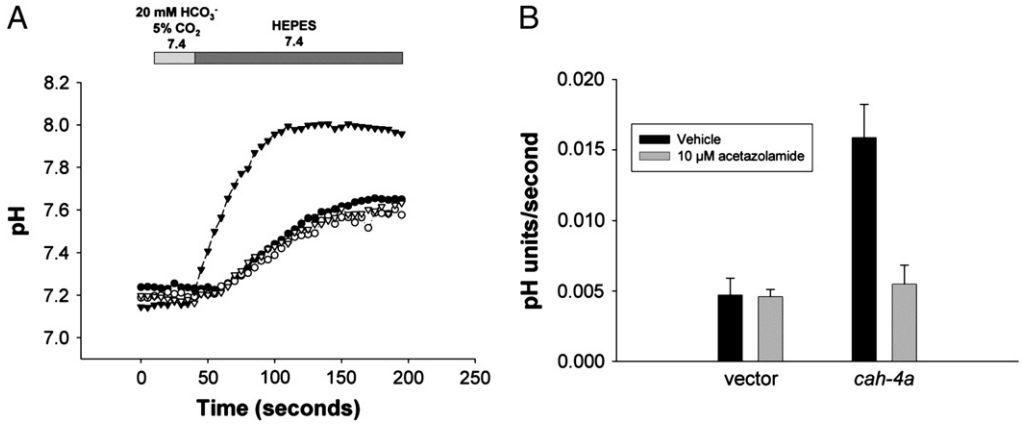

Fig. 6. CAH-4A accelerates pH changes that occur in the nucleus as a result of altering media CO_2 levels. (A) Representative traces of nuclear pH were obtained by dynamic fluorescent imaging of a SV40 NLS-targeted pH biosensor (Miesenbock ref. [36]) in cells that had been equilibrated in HCO_3^-/CO_2 media as they were switched to HCO_3^--free media. (B) The initial rate of ΔpH following perfusion with HCO_3^--free media was determined for six separate trials under each of the conditions shown. (●, vehicle; ○, acetazolamide;▼, *cah-4* + vehicle; ▽, *cah-4* + acetazolamide).

as well as head muscle cells (Fig. 3). The pan-neural expression suggests a potentially conserved function in these cells. Moreover, we and others have shown that CAH-4 isozymes are catalytically active (Fig. 5 and [29,30]). If catalytic activity is important for CAH-4A function, this would suggest that the nucleus is capable of responding to changes in HCO_3^-/CO_2 metabolism. In fact, recombinant CAH-4A exhibited clear nuclear activity when expressed in mammalian tissue culture cells (Fig. 5), and was capable of regulating nuclear pH in response to fluctuations in HCO_3^-/CO_2 (Fig. 6), as might be predicted for a catalytic CA targeted to the nucleus. It is unclear based solely upon this result however whether CAH-4A plays a role in endogenous nuclear pH regulation and similarly, how closely nuclear pH is tied to cytoplasmic pH. In fact, nuclear pH regulation is a relatively unexplored topic in general. It is likely that interrogating the physiologic role of CAH-4A in *C. elegans* will provide insight to these questions. In this regard, a genetic deletion of *cah-4* has been annotated as being lethal in its homozygous state (*cah-4*(*tm2805*)X; *C. elegans* Gene Knockout Consortium), clearly suggesting an important function for at least one of the two *cah-4* splice variants. Furthermore, we have observed that overexpressing CAH-4A in transgenic worms can lead to phenotypic abnormalities, including locomotor defects (data not shown), though the molecular basis for this dominant effect is currently unknown.

Interestingly, *cah-4* expression has been shown to be increased by hypoxia through the canonical HIF/VHL signaling pathway [31]. CAs are commonly regarded as cytoprotective enzymes, and HIF responsive genes generally promote survival under hypoxic conditions. For example, both mammalian CAIX and CAXII have been shown to be HIF responsive and are pro-survival factors. In particular, CAIX is highly expressed in multiple cancers, where it is used as a tumor marker. Mechanistically, CAIX is thought to facilitate acid diffusion and acid transport, thus contributing to tumor pH regulation (for review, see [52]). Moreover, a role for endogenous CAIX in neuronal maintenance was demonstrated by morphological analysis showing vacuolar degenerative changes in the brains of $Car9^{-/-}$ mice [53].

It has also been demonstrated that oxidative protein modification of CA isozymes, such as may occur under hypoxic conditions, is associated with disease pathophysiology. For example, protein carbonylation of CAII correlates with neuronal pathology in Alzheimer's disease [54] and carbonylation of CAIII contributes to oxidative deficiencies in muscle [55].

However, despite these observations of parallel regulatory motifs and the general underlying theme that CAs can modulate hypoxic sensitivity, there are no clear mammalian CAH-4 orthologs. As regards CAH-4A, none of the mammalian CAs has been shown to reside in the cell nucleus, nor do any of them contain a canonical nuclear localization signal. We suggest here that worm neurons are more exposed to environmental insults than mammalian neurons and that endogenous protective mechanisms in worms may have evolved into adaptive responses in mammals. This is consistent with the fact that worms are incredibly hypoxic resistant compared to mammals. Thus in the absence of a canonical nuclear CA in mammals, it is worth considering whether situational CA transport to the nucleus could occur, perhaps in response to stress signaling. Alternatively, stressors might induce the expression of a cryptic promoter or splice variant that encodes a nuclear CA isozyme.

Though not of the classical αCA family, in fact there has been one report of a protein capable of catalytic CA activity purified from the nucleus of mammalian cells. The protein was identified as NonO/p54nrb, and histochemical staining revealed CA activity in rat lymphocytes coincident with p54nrb expression [33]. p54nrb is associated with PSF (polypyrimidine-tract-binding-protein-associated splicing factor) and has been reported to be involved in diverse nuclear processes such as transcription, RNA processing, DNA unwinding and repair, and may contribute to the progression of malignant melanoma [56]. Whether CA activity contributes to any of these functions of p54nrb is currently unknown.

If a nuclear CA were catalytically active, our results suggest that it could contribute to nuclear pH regulation, and we predict that this might influence oxidative stress resistance. As alluded to above, however, there is not much known about nuclear pH regulation. Several reports have suggested that the pH of the nucleus is higher than that of the surrounding cytoplasm [57,58], but how this might occur mechanistically is unclear. Establishing a gradient between the cytoplasm and the nucleus would require either a barrier to the diffusion of protons or an extremely a fast enzyme that has H^+ or OH^- as a reaction component. CAH-4B was shown to have a Kcat/Km of $5.4\times10^7\ M^{-1}\ s^{-1}$ [30], which while not diffusion-limited is still second only to that of mammalian CAII.

Compartmentalization could also help to establish a nuclear pH microdomain. Although the nuclear pore should permit the free diffusion of small molecules such as electrolytes, there is compelling evidence that localized Ca^{2+} signaling within the nucleus occurs in response to synaptic activity, and this signaling elicits subsequent protective measures [59]. Protection occurs through altering the neuron's transcriptional profile [60] and may involve morphologic changes in the nucleus itself [61,62]. The observed alterations to nuclear geometry are consistent with the idea that the nucleoplasm is restricted into signaling microdomains. Since acid diffusion rates can be buffered by CA activity, microdomains may contribute to the ability of CAH-4A to regulate pH homeostasis in the nucleus.

However, the pK of DNA, while affected by base composition, is generally quite low, and the negative charge on the phosphate backbone of DNA will be largely unaffected by changes in pH in the physiologic range, Thus, it is unlikely that small changes in nuclear pH will have large effects on DNA binding to histones or transcription factors. It is possible that there is an alternative mechanism whereby pH might regulate nuclear function. Though pH is most commonly thought of as providing a metabolic context that shapes enzymatic activities in the cell, there is a growing notion that proton recognition may contribute directly to cell signaling [63–66]. It will be fascinating to determine whether CAH-4A contributes to nuclear pH homeostasis and whether the loss of CAH-4A has functional consequences on neuronal survival.

Acknowledgements

This work was supported in part by USPHS R01 NS064945 (K.N.) and a UNCF/Merck Postdoctoral Fellowship Award to T.A.M. We also acknowledge the *C. elegans* Genetics Center for strains.

Appendix A. Supplementary data

Supplementary data to this article can be found online at doi:10.1016/j.bbamcr.2011.12.014.

References

[1] A. Aspatwar, M.E. Tolvanen, S. Parkkila, Phylogeny and expression of carbonic anhydrase-related proteins, BMC Mol. Biol. 11 (2010) 25.
[2] W.S. Sly, P.Y. Hu, Human carbonic anhydrases and carbonic anhydrase deficiencies, Annu. Rev. Biochem. 64 (1995) 375–401.
[3] S. Saari, M. Hilvo, P. Pan, G. Gros, N. Hanke, A. Waheed, W.S. Sly, S. Parkkila, The most recently discovered carbonic anhydrase, CA XV, is expressed in the thick ascending limb of Henle and in the collecting ducts of mouse kidney, PLoS One 5 (2010) e9624.
[4] M. Schultz, W. Jin, A. Waheed, B.R. Moed, W. Sly, Z. Zhang, Expression profile of carbonic anhydrases in articular cartilage, Histochem. Cell Biol. 136 (2011) 145–151.
[5] C.T. Supuran, Carbonic anhydrases—an overview, Curr. Pharm. Des. 14 (2008) 603–614.
[6] D. Sterling, B.V. Alvarez, J.R. Casey, The extracellular component of a transport metabolon. Extracellular loop 4 of the human AE1 Cl^-/HCO_3^- exchanger binds carbonic anhydrase IV, J. Biol. Chem. 277 (2002) 25239–25246.
[7] F.B. Loiselle, P.E. Morgan, B.V. Alvarez, J.R. Casey, Regulation of the human NBC3 Na+/HCO3− cotransporter by carbonic anhydrase II and PKA, Am. J. Physiol. Cell Physiol. 286 (2004) C1423–C1433.

[8] P.E. Morgan, C.T. Supuran, J.R. Casey, Carbonic anhydrase inhibitors that directly inhibit anion transport by the human $Cl^-/HCO3^-$ exchanger, AE1, Mol. Membr. Biol. 21 (2004) 423–433.
[9] B.V. Alvarez, G.L. Vilas, J.R. Casey, Metabolon disruption: a mechanism that regulates bicarbonate transport, EMBO J. 24 (2005) 2499–2511.
[10] P.E. Morgan, S. Pastorekova, A.K. Stuart-Tilley, S.L. Alper, J.R. Casey, Interactions of transmembrane carbonic anhydrase, CAIX, with bicarbonate transporters, Am. J. Physiol. Cell Physiol. 293 (2007) C738–C748.
[11] W.S. Sly, D. Hewett-Emmett, M.P. Whyte, Y.S. Yu, R.E. Tashian, Carbonic anhydrase II deficiency identified as the primary defect in the autosomal recessive syndrome of osteopetrosis with renal tubular acidosis and cerebral calcification, Proc. Natl. Acad. Sci. U. S. A. 80 (1983) 2752–2756.
[12] G.N. Shah, B. Ulmasov, A. Waheed, T. Becker, S. Makani, N. Svichar, M. Chesler, W.S. Sly, Carbonic anhydrase IV and XIV knockout mice: roles of the respective carbonic anhydrases in buffering the extracellular space in brain, Proc. Natl. Acad. Sci. U. S. A. 102 (2005) 16771–16776.
[13] N. Svichar, A. Waheed, W.S. Sly, J.C. Hennings, C.A. Hubner, M. Chesler, Carbonic anhydrases CA4 and CA14 both enhance AE3-mediated Cl^-HCO3^- exchange in hippocampal neurons, J. Neurosci. 29 (2009) 3252–3258.
[14] M. Pasternack, S. Smirnov, K. Kaila, Proton modulation of functionally distinct GABAA receptors in acutely isolated pyramidal neurons of rat hippocampus, Neuropharmacology 35 (1996) 1279–1288.
[15] U. Bonnet, T. Leniger, M. Wiemann, Alteration of intracellular pH and activity of CA3-pyramidal cells in guinea pig hippocampal slices by inhibition of transmembrane acid extrusion, Brain Research 872 (2000) 116–124.
[16] M. Klier, C. Schuler, A.P. Halestrap, W.S. Sly, J.W. Deitmer, H.M. Becker, Transport activity of the high-affinity monocarboxylate transporter MCT2 is enhanced by extracellular carbonic anhydrase IV but not by intracellular carbonic anhydrase II, J. Biol. Chem. 286 (2011) 27781–27791.
[17] Z. Yang, B.V. Alvarez, C. Chakarova, L. Jiang, G. Karan, J.M. Frederick, Y. Zhao, Y. Sauve, X. Li, E. Zrenner, B. Wissinger, A.I.D. Hollander, B. Katz, W. Baehr, F.P. Cremers, J.R. Casey, S.S. Bhattacharya, K. Zhang, Mutant carbonic anhydrase 4 impairs pH regulation and causes retinal photoreceptor degeneration, Hum. Mol. Genet. 14 (2005) 255–265.
[18] J.A. Loncaster, A.L. Harris, S.E. Davidson, J.P. Logue, R.D. Hunter, C.C. Wycoff, J. Pastorek, P.J. Ratcliffe, I.J. Stratford, C.M. West, Carbonic anhydrase (CA IX) expression, a potential new intrinsic marker of hypoxia: correlations with tumor oxygen measurements and prognosis in locally advanced carcinoma of the cervix, Cancer Res. 61 (2001) 6394–6399.
[19] C.C. Wykoff, N.J. Beasley, P.H. Watson, K.J. Turner, J. Pastorek, A. Sibtain, G.D. Wilson, H. Turley, K.L. Talks, P.H. Maxwell, C.W. Pugh, P.J. Ratcliffe, A.L. Harris, Hypoxia-inducible expression of tumor-associated carbonic anhydrases, Cancer Res. 60 (2000) 7075–7083.
[20] M.H. Bui, D. Seligson, K.R. Han, A.J. Pantuck, F.J. Dorey, Y. Huang, S. Horvath, B.C. Leibovich, S. Chopra, S.Y. Liao, E. Stanbridge, M.I. Lerman, A. Palotie, R.A. Figlin, A.S. Belldegrun, Carbonic anhydrase IX is an independent predictor of survival in advanced renal clear cell carcinoma: implications for prognosis and therapy, Clin. Cancer Res. 9 (2003) 802–811.
[21] J.R. Turner, R.D. Odze, C.P. Crum, M.B. Resnick, MN antigen expression in normal, preneoplastic, and neoplastic esophagus: a clinicopathological study of a new cancer-associated biomarker, Hum. Pathol. 28 (1997) 740–744.
[22] J. Saarnio, S. Parkkila, A.K. Parkkila, K. Haukipuro, S. Pastorekova, J. Pastorek, M.I. Kairaluoma, T.J. Karttunen, Immunohistochemical study of colorectal tumors for expression of a novel transmembrane carbonic anhydrase, MN/CA IX, with potential value as a marker of cell proliferation, Am. J. Pathol. 153 (1998) 279–285.
[23] Y. Li, H. Wang, E. Oosterwijk, Y. Selman, J.C. Mira, T. Medrano, K.T. Shiverick, S.C. Frost, Antibody-specific detection of CAIX in breast and prostate cancers, Biochem. Biophys. Res. Commun. 386 (2009) 488–492.
[24] J.Y. Winum, A. Scozzafava, J.L. Montero, C.T. Supuran, Inhibition of carbonic anhydrase IX: a new strategy against cancer, Anticancer Agents in Medicinal Chemistry 9 (2009) 693–702.
[25] I.P. Kaur, R. Smitha, D. Aggarwal, M. Kapil, Acetazolamide: future perspective in topical glaucoma therapeutics, Int. J. Pharm. 248 (2002) 1–14.
[26] W.G. Reiss, K.S. Oles, Acetazolamide in the treatment of seizures, Ann. Pharmacother. 30 (1996) 514–519.
[27] H.G. Sullivan, T.B.t. Kingsbury, M.E. Morgan, R.D. Jeffcoat, J.D. Allison, J.J. Goode, D.E. McDonnell, The rCBF response to Diamox in normal subjects and cerebrovascular disease patients, J. Neurosurg. 67 (1987) 525–534.
[28] C.K. Grissom, R.C. Roach, F.H. Sarnquist, P.H. Hackett, Acetazolamide in the treatment of acute mountain sickness: clinical efficacy and effect on gas exchange, Ann. Intern. Med. 116 (1992) 461–465.
[29] M.K. Fasseas, D. Tsikou, E. Flemetakis, P. Katinakis, Molecular and biochemical analysis of the alpha class carbonic anhydrases in *Caenorhabditis elegans*, Mol. Biol. Rep. 38 (2011) 1777–1785.
[30] R.A. Hall, D. Vullo, A. Innocenti, A. Scozzafava, C.T. Supuran, P. Klappa, F.A. Muhlschlegel, External pH influences the transcriptional profile of the carbonic anhydrase, CAH-4b in *Caenorhabditis elegans*, Mol. Biochem. Parasitol. 161 (2008) 140–149.
[31] T. Bishop, K.W. Lau, A.C. Epstein, S.K. Kim, M. Jiang, D. O'Rourke, C.W. Pugh, J.M. Gleadle, M.S. Taylor, J. Hodgkin, P.J. Ratcliffe, Genetic analysis of pathways regulated by the von Hippel–Lindau tumor suppressor in *Caenorhabditis elegans*, PLoS Biology 2 (2004) e289.
[32] J. Giacomotto, C. Pertl, C. Borrel, M.C. Walter, S. Bulst, B. Johnsen, D.L. Baillie, H. Lochmuller, C. Thirion, L. Segalat, Evaluation of the therapeutic potential of carbonic anhydrase inhibitors in two animal models of dystrophin deficient muscular dystrophy, Hum. Mol. Genet. 18 (2009) 4089–4101.
[33] P. Karhumaa, S. Parkkila, A. Waheed, A.K. Parkkila, K. Kaunisto, P.W. Tucker, C.J. Huang, W.S. Sly, H. Rajaniemi, Nuclear NonO/p54(nrb) protein is a nonclassical carbonic anhydrase, J. Biol. Chem. 275 (2000) 16044–16049.
[34] C.C. Mello, J.M. Kramer, D. Stinchcomb, V. Ambros, Efficient gene transfer in *C. elegans*: extrachromosomal maintenance and integration of transforming sequences, EMBO J. 10 (1991) 3959–3970.
[35] K. Nehrke, A reduction in intestinal cell pHi due to loss of the *Caenorhabditis elegans* $Na+/H+$ exchanger NHX-2 increases life span, J. Biol. Chem. 278 (45) (2003) 44657–44666.
[36] G. Miesenbock, D.A. De Angelis, J.E. Rothman, Visualizing secretion and synaptic transmission with pH-sensitive green fluorescent proteins, Nature 394 (1998) 192–195.
[37] J.A. Thomas, R.N. Buchsbaum, A. Zimniak, E. Racker, Intracellular pH measurements in Ehrlich ascites tumor cells utilizing spectroscopic probes generated in situ, Biochemistry 18 (1979) 2210–2218.
[38] H.P. Hansson, Histochemical demonstration of carbonic anhydrase activity, Histochemie 11 (1967) 112–128.
[39] N. Fabre, I.M. Reiter, N. Becuwe-Linka, B. Genty, D. Rumeau, Characterization and expression analysis of genes encoding alpha and beta carbonic anhydrases in Arabidopsis, Plant Cell Environ. 30 (2007) 617–629.
[40] R.E. Tashian, The carbonic anhydrases: widening perspectives on their evolution, expression and function, Bioessays 10 (1989) 186–192.
[41] S.A. Hazen, A. Waheed, W.S. Sly, K.F. LaNoue, C.J. Lynch, Differentiation-dependent expression of CA V and the role of carbonic anhydrase isozymes in pyruvate carboxylation in adipocytes, FASEB J. 10 (1996) 481–490.
[42] S.J. Dodgson, Why are there carbonic anhydrases in the liver? Biochem. Cell Biol. 69 (1991) 761–763.
[43] D.J. Culp, B. Robinson, S. Parkkila, P.W. Pan, M.N. Cash, H.N. Truong, T.W. Hussey, S.L. Gullett, Oral colonization by Streptococcus mutans and caries development is reduced upon deletion of carbonic anhydrase VI expression in saliva, Biochim. Biophys. Acta 1812 (2011) 1567–1576.
[44] M. Kimoto, M. Kishino, Y. Yura, Y. Ogawa, A role of salivary carbonic anhydrase VI in dental plaque, Arch. Oral Biol. 51 (2006) 117–122.
[45] B. Elleby, B. Sjoblom, C. Tu, D.N. Silverman, S. Lindskog, Enhancement of catalytic efficiency by the combination of site-specific mutations in a carbonic anhydrase-related protein, Eur. J. Biochem. 267 (2000) 5908–5915.
[46] B. Sjoblom, B. Elleby, K. Wallgren, B.-H. Jonsson, S. Lindskog, Two point mutations convert a catalytically inactive carbonic anhydrase-related protein (CARP) to an active enzyme, FEBS Lett. 398 (1996) 322–325.
[47] E. Miyaji, I. Nishimori, K. Taniuchi, T. Takeuchi, Y. Ohtsuki, S. Onishi, Overexpression of carbonic anhydrase-related protein VIII in human colorectal cancer, J. Pathol. 201 (2003) 37–45.
[48] Y. Jiao, J. Yan, Y. Zhao, L.R. Donahue, W.G. Beamer, X. Li, B.A. Roe, M.S. Ledoux, W. Gu, Carbonic anhydrase-related protein VIII deficiency is associated with a distinctive lifelong gait disorder in waddles mice, Genetics 171 (2005) 1239–1246.
[49] M. Hirasawa, X. Xu, R.B. Trask, T.P. Maddatu, B.A. Johnson, J.K. Naggert, P.M. Nishina, A. Ikeda, Carbonic anhydrase related protein 8 mutation results in aberrant synaptic morphology and excitatory synaptic function in the cerebellum, Mol. Cell. Neurosci. 35 (2007) 161–170.
[50] J. Hirota, H. Ando, K. Hamada, K. Mikoshiba, Carbonic anhydrase-related protein is a novel binding protein for inositol 1,4,5-trisphosphate receptor type 1, Biochem. J. 372 (2003) 435–441.
[51] A.J. Bretscher, E. Kodama-Namba, K.E. Busch, R.J. Murphy, Z. Soltesz, P. Laurent, M. de Bono, Temperature, oxygen, and salt-sensing neurons in *C. elegans* are carbon dioxide sensors that control avoidance behavior, Neuron 69 (2011) 1099–1113.
[52] P. Swietach, A. Hulikova, R.D. Vaughan-Jones, A.L. Harris, New insights into the physiological role of carbonic anhydrase IX in tumour pH regulation, Oncogene 29 (2010) 6509–6521.
[53] P.W. Pan, A.K. Parkkila, S. Autio, M. Hilvo, R. Sormunen, S. Pastorekova, J. Pastorek, H. Haapasalo, S. Parkkila, Brain phenotype of carbonic anhydrase IX-deficient mice, Transgenic Res. 21 (2012) 163–176.
[54] R. Sultana, M. Perluigi, S.F. Newman, W.M. Pierce, C. Cini, R. Coccia, D.A. Butterfield, Redox proteomic analysis of carbonylated brain proteins in mild cognitive impairment and early Alzheimer's disease, Antioxid. Redox Signal. 12 (2010) 327–336.
[55] E. Barreiro, S.N. Hussain, Protein carbonylation in skeletal muscles: impact on function, Antioxid. Redox Signal. 12 (2010) 417–429.
[56] S. Schiffner, N. Zimara, R. Schmid, A.K. Bosserhoff, p54nrb is a new regulator of progression of malignant melanoma, Carcinogenesis 32 (2011) 1176–1182.
[57] O. Seksek, J. Bolard, Nuclear pH gradient in mammalian cells revealed by laser microspectrofluorimetry, J. Cell Sci. 109 (1996) 257–262.
[58] J. Llopis, J.M. McCaffery, A. Miyawaki, M.G. Farquhar, R.Y. Tsien, Measurement of cytosolic, mitochondrial, and Golgi pH in single living cells with green fluorescent proteins, Proc. Natl. Acad. Sci. U. S. A. 95 (1998) 6803–6808.
[59] S. Papadia, P. Stevenson, N.R. Hardingham, H. Bading, G.E. Hardingham, Nuclear $Ca2+$ and the cAMP response element-binding protein family mediate a late phase of activity-dependent neuroprotection, J. Neurosci. 25 (2005) 4279–4287.
[60] S.J. Zhang, M. Zou, L. Lu, D. Lau, D.A. Ditzel, C. Delucinge-Vivier, Y. Aso, P. Descombes, H. Bading, Nuclear calcium signaling controls expression of a large gene pool: identification of a gene program for acquired neuroprotection induced by synaptic activity, PLoS Genet. 5 (2009) e1000604.
[61] G. Queisser, S. Wiegert, H. Bading, Structural dynamics of the cell nucleus: basis for morphology modulation of nuclear calcium signaling and gene transcription, Nucleus 2 (2011) 98–104.

[62] M. Wittmann, G. Queisser, A. Eder, J.S. Wiegert, C.P. Bengtson, A. Hellwig, G. Wittum, H. Bading, Synaptic activity induces dramatic changes in the geometry of the cell nucleus: interplay between nuclear structure, histone H3 phosphorylation, and nuclear calcium signaling, J. Neurosci. 29 (2009) 14687–14700.
[63] J. Pfeiffer, D. Johnson, K. Nehrke, Oscillatory transepithelial H(+) flux regulates a rhythmic behavior in *C. elegans*, Curr. Biol. 18 (2008) 297–302.
[64] M.A. Kader, S. Lindberg, Cytosolic calcium and pH signaling in plants under salinity stress, Plant Signal. Behav. 5 (2010) 233–238.
[65] A.A. Beg, G.G. Ernstrom, P. Nix, M.W. Davis, E.M. Jorgensen, Protons act as a transmitter for muscle contraction in *C. elegans*, Cell 132 (2008) 149–160.
[66] M. Sandoval, J. Burgos, F.V. Sepulveda, L.P. Cid, Extracellular pH in restricted domains as a gating signal for ion channels involved in transepithelial transport, Biol. Pharm. Bull. 34 (2011) 803–809.